How to Cite: Houbi, A., Zharmenov, A.A., Atassi, Y., Bagasharova, Z.T., Mirzalieva, S., & Karibayev, B.A. (2022) Synthesis and Microwave Absorption Properties of $Ni_{0.5}Zn_{0.5}Fe_2O_4$/CI Composite Coated with Polyaniline within Paraffin Wax Matrix. *Bulletin of the University of Karaganda – Chemistry, 107(3), 254-266.* https://doi.org/10.31489/2022Ch3/3-22-8

Article Received: 19 May 2022 | Revised: 29 June 2022 | Accepted: 11 July 2022 | Published online: 20 July 2022

UDC 542.943 https://doi.org/10.31489/2022Ch3/3-22-8

A. Houbi[1, 2*], A.A. Zharmenov[1, 2], Y. Atassi[3],
Z.T. Bagasharova[1, 2], S. Mirzalieva[1, 2], B.A. Karibayev[4]

[1]*National Center on Complex Processing of Mineral Raw Materials of the Republic of Kazakhstan, Almaty, Kazakhstan;*
[2]*Department of Chemical Technology of Inorganic Substances, Al-Farabi Kazakh National University, Almaty, Kazakhstan;*
[3]*Department of Applied Physics, Higher Institute for Applied Sciences and Technology, Damascus, Syria;*
[4]*Department of Physics and Technology, Al-Farabi Kazakh National University, Almaty, Kazakhstan*
([*]Corresponding author's e-mail: Anashoubi@gmail.com)

Synthesis and Microwave Absorption Properties of $Ni_{0.5}Zn_{0.5}Fe_2O_4$/CI Composite Coated with Polyaniline within Paraffin Wax Matrix

Ternary composites of polyaniline/$Ni_{0.5}Zn_{0.5}Fe_2O_4$/carbonyl iron (PANI/F/CI) are prepared via two stages. Firstly, $Ni_{0.5}Zn_{0.5}Fe_2O_4$ is prepared using a sol-gel method. After that, PANI/F/CI composites are prepared using an in-situ polymerization technique of PANI in the existence of the $Ni_{0.5}Zn_{0.5}Fe_2O_4$ and CI. X-ray diffractometry (XRD), Fourier transform infrared (FTIR) spectroscopy, Ultraviolet-visible (UV-vis) spectroscopy, and Thermogravimetric analysis (TGA) are utilized to characterize samples. The morphology of the powders is investigated by Scanning electron microscope (SEM). The electromagnetic interference (EMI) shielding and microwave absorption (MA) properties are measured in the frequency band of 8.8–12 GHz to investigate the microwave characterization. The results refer those microwave absorption properties are related to the absorber thickness and the loading ratio of the absorber within a paraffin matrix. Minimal reflection loss of –30.8 dB at the matching frequency (f_m) of 10.3 GHz and the absorption bandwidth under –10 dB (BW_{-10dB}) of 2.8 GHz for 3.4 mm thickness with a surface density (SD) of 3.38 kg/m^2 are noticed for the PANI/F/CI composite sample. The maximum shielding efficiency (SE) of 30.12 dB at 11.0 GHz for 3.2 mm thickness is observed for the PANI/F/CI composite sample.

Keywords: polyaniline, carbonyl iron, composites, lightweight microwave absorber, reflection loss, absorption bandwidth, shielding efficiency, matching frequency.

Introduction

Recent environmental pollution issues are appearing because of the quick evolution of electronic devices, involving smartphones, laptops, and intelligent devices. Electronic apparatuses emit undesirable EM waves, generating electromagnetic interference between various electronic apparatuses with a negative effect on their performance. Consequently, the disposal of EM waves resulting from EMI effectively is so important both for public protection security and electronic safety. Generally, there are two kinds of materials to absorb EM waves: firstly, magnetic loss materials such as hexagonal ferrites, spinel ferrites, and carbonyl iron, secondly, dielectric loss materials such as conductive polymers (e.g., polyaniline, polypyrrole) and carbonaceous materials (e.g., carbon black, activated carbon, carbon fibers, graphene) which have played a significant role for high-frequency EM wave absorption. Nevertheless, the drawbacks involving elevated density, low reflection absorption, and narrow wideband have hugely limited conventional loss materials' workable benefits for EM wave absorption [1, 2]. In recent years, microwave absorption composites based on polyaniline, ferrite, and carbonyl iron have obtained significant attention due to their excellent electrical and ferrimagnetic characteristics. Polyaniline-based composites have pulled in major attention for microwave absorption lately. Polyaniline is usually used to fit the requirements of high-effective microwave attenuation materials because of its superior characteristics, for example, low density, high permittivity, unique electronic conductivity, etc. Polyaniline has a unique place in the band of elevated-frequency microwave absorption materials (MAMs). Furthermore, spinel ferrites and carbonyl iron have excellent MA characteristics due to their unique magnetic characteristics. NiZn ferrites and carbonyl iron are considered suitable materials for high-frequency implementations [3, 4]. When NiZn ferrite and carbonyl iron are mixed with Polyaniline, the MA characteristics of the resultant composite are anticipated to enhance. According to this, PANI/NiZn ferrite microwave absorbers in the frequency range of 2–40 GHz were successfully prepared by Ting et al. [3].

The absorbers are prepared by dispersing PANI/NiZn ferrite nanocomposites with a weight ratio of 67% w/w within an epoxy resin matrix. The results indicated that by increasing polyaniline content in NiZn ferrite, a wide absorption frequency range could be obtained. Didehban et al. have designed microwave absorbers in the frequency band of 8–12 GHz based on NiZn ferrite-PANI (35:65) nanocomposites. The absorbers are formed by dispersing PANI/NiZn ferrite within an epoxy resin matrix of 20 w/w. The results have shown that the absorber had a RL_{min} of –20 dB at 9.1 GHz and the absorption BW_{-10dB} was 0.5 GHz for 2 mm thickness [5]. Wang et al. have designed absorbers in the frequency band of 2–8 GHz based on NiZn Ferrite/PANI (1:3) nanocomposites. The absorbers are formed by dispersing PANI/NiZn ferrite within a paraffin matrix of 75 w/w. The absorbers were papered by the in-situ polymerization method. The results displayed that RL_{min} was –32 dB at 9.5 GHz and the absorption $B.W_{-10\ dB}$ was 3.8 GHz [6]. Wang et al. have reported the MA properties of a one-dimensional uniform PANI/NiZn ferrite hybrid nanorods within a paraffin matrix of 70 % w/w in the frequency range of 2–18 GHz. They have found that the absorbers had broadband, and minimal reflection loss, where the results have indicated that the absorber had a RL_{min} of –27.5 dB at 6.2 GHz and the absorption BW_{-10dB} was 3 GHz for 2 mm thickness [7]. Wang et al. have designed absorbers in the frequency band of 2–18 GHz based on NiZn Ferrite/PANI nanocomposites. The absorbers were papered by hydrothermal method. The results displayed that RL_{min} was –17 dB at 11.1 GHz and the absorption $B.W_{-10\ dB}$ was 5 GHz [8]. Ma et al. have reported the MA properties of PANI/$Co_{0.5}Zn_{0.5}Fe_2O_4$ nanocomposite. The MA properties were studied in the 8.2-26.5 GHz range. The absorbers were synthesized by the in-situ polymerization technique. They have found that the absorbers had broadband, and minimal reflection loss, where the results have indicated that the absorber had a RL_{min} of –39.9 dB at 22.4 GHz and the absorption BW_{-10dB} was 5 GHz for 2 mm thickness [9].

The aim of the study is to design lightweight and wide band absorbers with loading ratios not exceeding 35% with enhanced RL based on PANI/F/CI nanocomposites. The ferrite is prepared by the sol-gel method. Then, the aniline monomer is polymerized by the in-situ polymerization technique in the presence of NiZn ferrite and carbonyl iron. The prepared samples are characterized by XRD, FTIR spectroscopy, UV-vis spectroscopy and TGA. The morphologies of the ferrite and its nanocomposites are identified using SEM. The EMI shielding and MA properties are studied by measuring the minimal reflection loss, absorption bandwidth under -10 dB, and shielding efficiency of the absorbers in the frequency band of 8.8–12 GHz to achieve functional characterization. To the best of the authors' knowledge, the optimization of the performance of the current PANI/F/CI nanocomposites in terms of lightweight and wide bandwidth has not been reported before.

Experimental

Chemicals: Sodium dodecyl sulfate (SDS, 92.2 % purity), ammonium persulfate (APS, 95.3 % purity), nickel (II) nitrate hexahydrate ($Ni(NO_3)_2{\cdot}6H_2O$, 98.3 % purity), zinc nitrate hexahydrate ($Zn(NO_3)_2{\cdot}6\,H_2O$, 98.7% purity), and iron (III) nitrate nonahydrate ($Fe(NO_3)_3{\cdot}9H_2O$, 98.2 % purity) were purchased from TRADING COMPANY ANT, Russia. As well, Aniline monomer ($C_6H_5NH_2$, 99.5 % purity), Ammonium hydroxide (NH_4OH, 99.8 % purity), Citric acid ($C_6H_8O_7$, 99.0% purity) were purchased from Sigma Aldrich Company, Germany. On the other hand, carbonyl iron (CI, 99.6% purity) was purchased from Cabot Norit Company, Netherland.

Instruments used: A powder X-ray diffractometer (XRD, Rigaku Miniflex 600, Cu-Ka) is utilized for defining the crystal structures of the powders. Fourier Transform IR (FTIR) spectra are recorded on a Perkin Elmer spectrum 65 FTIR spectrometer in the range of 400–4000 cm^{-1}. The UV-vis absorption spectra of the samples (dispersed in dimethylformamide (DMF)) are recorded using the LAMBDA 365 UV-vis spectrophotometer in the range of 250–900 nm. Thermogravimetric analysis (TGA) is done utilizing a thermal analyzer (NETZSCH 449F3A-0372-M) under a nitrogen atmosphere, from room temperature to 1000 °C under constant heating rate of 10 °C/min. A scanning electron microscope (FEI Quanta 200 3D) is utilized for defining the morphology of the powders. Finally, energy-dispersive X-ray spectroscopy (EDX, Quanta 200 3D) is utilized to know the chemical composition of prepared samples.

The microwave absorption properties of the prepared samples are calculated by using the horn antenna connected to an oscilloscope (AKTAKOM ADS-2221M).

Methodology

1. Preparation of PANI/F/CI

Ferrite ($Ni_{0.5}Zn_{0.5}Fe_2O_4$) nanoparticles were prepared by a sol-gel method as illustrated in the following literature [10–14]. On the other hand, carbonyl iron powder was milled for 12 h at 300 rpm via the grinding balls to obtain fine powders. NiZn ferrite and carbonyl iron were coated with polyaniline via the in-situ polymerization technique. Firstly, 6 g (90 % F and 10 % CI) was added to 100 ml distilled water under mechanical stirring at a speed of 250 rpm for 30 minutes. 3 g sodium dodecyl sulfate (SDS) and aniline were added to the solution while keeping mechanical stirring for 1 h. After that, 1 M HCl solution 80 mL was added to the solution under stirring for 1 h. Finally, 8.5 g APS was dissolved in 100 ml of an aqueous solution which was utilized as an oxidizing agent and added slowly dropwise into the solution to start the polymerization. The polymerization was allowed to proceed for 6 h with stirring in an ice bath. The resulting composite was filtered and washed many times with distilled water and ethanol, and then dried for 8 h in the furnace at 70 °C. The weight ratio of aniline/(F-CI) (1/1) was synthesized. Pure polyaniline was synthesized in a similar way but without NiZn ferrite and carbonyl iron solution for comparison purposes.

2. Preparation of samples for measuring the MA and EMI shielding properties

Microwave absorption and electromagnetic interference shielding properties of the samples were estimated with the free-space technique. According to this, 30–35 % w/w of the coated composites were dispersed in a paraffin wax matrix by heating and stirring for 15 min. Thereafter, the single-layer samples were molded to the dimensions of 100×100 mm to measure RL and SE in the frequency band of 8.8–12 GHz.

Results and Discussion

XRD patterns

Figure 1 demonstrates the XRD patterns of $Ni_{0.5}Zn_{0.5}Fe_2O_4$, CI, PANI/F/CI composite and PANI. For the $Ni_{0.5}Zn_{0.5}Fe_2O_4$ pattern, six diffraction peaks are noticed at 2θ values of 30.04°, 35.44°, 43.12°, 53.68°, 57.18°, and 62.14°, which conforms to (hkl) planes of (220), (311), (400), (422), (511) and (440), respectively. The ideal spinel structure is noticed by the peaks of NiZn ferrite [15]. The XRD pattern of $Ni_{0.5}Zn_{0.5}Fe_2O_4$ is matched with the reference XRD patterns (JCPDS, PDF no. 08–0234). The size of the NiZn ferrite grain (2θ =35.44°) has been evaluated with Scherrer's equation, $D = 0.9\ \lambda/\beta \cos\theta$, where D is the crystallite size (nm), λ is the X-ray wavelength, β is the bandwidth at half-height, and θ is the diffraction angle in degree. The calculated crystallite size of the NiZn ferrite is 27.6 nm. On the other hand, for the carbonyl iron pattern, three characteristic peaks are noticed at 2θ values of 44.61°, 64.92° and 82.33°, which conform to (hkl) planes of (100), (200), and (211), respectively. The XRD pattern of carbonyl iron resembles crystallites in which the sample mainly contains α-Fe phase [16]. All the observed peaks of CI are matched with the standard XRD pattern (JCPDS, PDF no. 06-0696). The characteristic peaks of the PANI/F/CI composite show matching the characteristic peaks of $Ni_{0.5}Zn_{0.5}Fe_2O_4$ as mentioned above. The XRD pattern of the pure PANI (Figure 1) displays an amorphous structure with two characteristic peaks at 20.22° and 25.36° which are attributed to the periodicity parallel to the polymer chains of PANI [17,18]. The XRD patterns of the PANI/F/CI composite (Figure 1) display crystalline peaks because of the existence of NiZn ferrite in this composite. The two characteristic peaks of the PANI disappeared due to the $Ni_{0.5}Zn_{0.5}Fe_2O_4$ nanoparticles [19, 20].

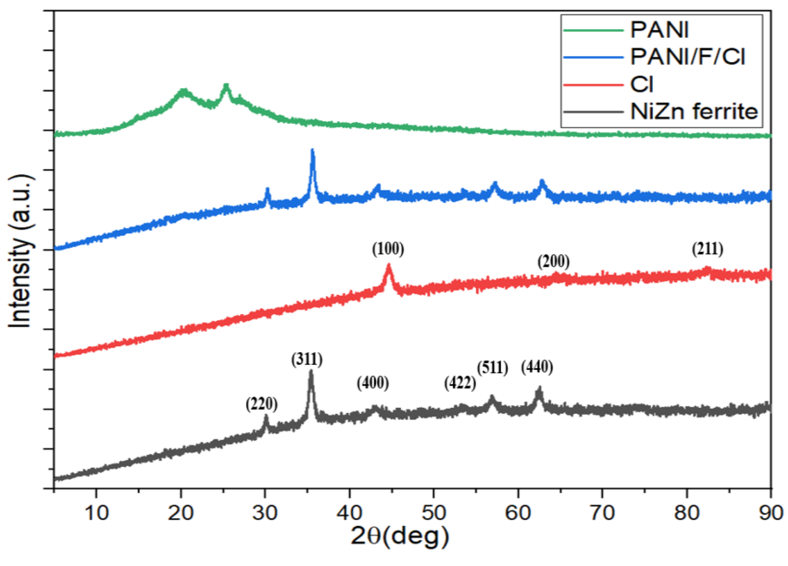

Figure 1. XRD patterns of $Ni_{0.5}Zn_{0.5}Fe_2O_4$, CI, PANI/F/CI composite and pure PANI

FTIR spectra

Figure 2 shows the FTIR spectra of the $Ni_{0.5}Zn_{0.5}Fe_2O_4$, CI, PANI/F/CI composite and PANI. For the $Ni_{0.5}Zn_{0.5}Fe_2O_4$ nanoparticles, two peaks at 563.1 cm^{-1} and 430.2 cm^{-1} are referring to the stretching vibration of (Fe–O), which emphasizes the formation of the metal-oxygen in ferrite-based [21]. In addition to that, the peak at 1630.4 cm^{-1} in $Ni_{0.5}Zn_{0.5}Fe_2O_4$, and CI is referring to C=O stretching vibration, and the peaks at 2348 cm^{-1} and 3452 cm^{-1} are referring to O–H stretching vibration [22, 23]. On the other hand, the characteristic peaks of PANI and PANI/F/CI composite are similar and they exhibited peaks at 1568 cm^{-1}, 1489 cm^{-1}, 1298 cm^{-1}, 1238 cm^{-1}, 1113 cm^{-1}, and 800 cm^{-1} [24, 25]. The characteristic peaks at 1568 and 1489 cm^{-1} are attributed to the C=N and C=C stretching modes of vibration for the quinonoid and benzenoid units of the polymer. The characteristic peaks at 1298 and 1238 cm^{-1} are related to N–H bending and asymmetric C–H stretching of the benzenoid ring, respectively. Finally, the characteristic peaks at 1113 cm^{-1} and 800 cm^{-1} are ascribed to the vibration mode of N=Q=N and the out-of-plane stretching vibration of C–H, respectively [19, 20]. In addition to that, the characteristic peak at 563.1 cm^{-1} of PANI/F/CI composite shows matching the characteristic peak of $Ni_{0.5}Zn_{0.5}Fe_2O_4$ as mentioned above. This indicates the stretching vibration of (Fe–O), which confirms the formation of the metal-oxygen in PANI/F/CI.

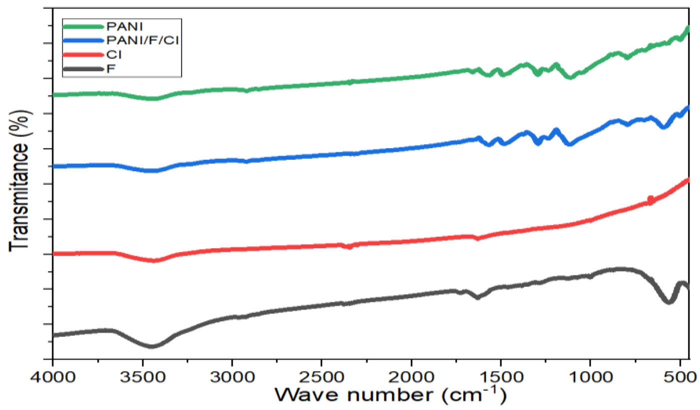

Figure 2. FTIR spectra of $Ni_{0.5}Zn_{0.5}Fe_2O_4$, CI, PANI/F/CI composite and pure PANI

UV-visible spectra

Figure 3 illustrates the UV–visible spectrum of the PANI and PANI/F/CI composite. For PANI, two characteristic peaks at around 302 nm and 629 nm are observed. The characteristic peak around 302 nm is ascribed to π–π* transition of the benzenoid ring and the characteristic peak around 629 nm is attributed to the benzenoid-to-quinoid excitonic transition [17, 26]. It can be seen that the characteristic peaks of PANI/F/CI composite show a clear red shift of 7 nm, as compared with that of polyaniline. The two characteristic peaks show the presence of PANI on the surface of $Ni_{0.5}Zn_{0.5}Fe_2O_4$ and carbonyl iron. These results may refer to the σ–π interaction among $Ni_{0.5}Zn_{0.5}Fe_2O_4$, carbonyl iron and polyaniline backbone, which leads to the energy of the antibonding orbital decrease, the energy of the π–π* transition of the benzenoid and quinoid ring decreases, so the characteristic peaks of the composite show a red shift [26].

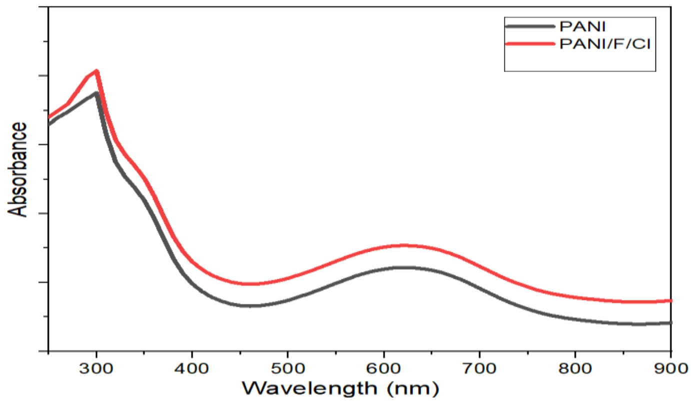

Figure 3. UV spectra of PANI and PANI/F/CI composite.

TGA analysis

Figure 4 shows the TGA curves of the $Ni_{0.5}Zn_{0.5}Fe_2O_4$, PANI/F/CI composite and PANI. For the $Ni_{0.5}Zn_{0.5}Fe_2O_4$ nanoparticles, no mass loss was noticed over the whole temperature range. PANI loses 4.87 % of its weight in the range of 110–130 °C because of the evaporation of moisture in the PANI. The thermal decomposition of the PANI is shown in the range of 230–1000 °C and has a big weight loss of 65.12 %. On the other hand, PANI/F/CI composite loses about 2.21 % of its weight in the range of 110–130 °C which is due to the evaporation of moisture in the composite. The thermal decomposition of the PANI/F/CI composite is shown in the range of 240–870 °C and has a big weight loss of 46.28 %.

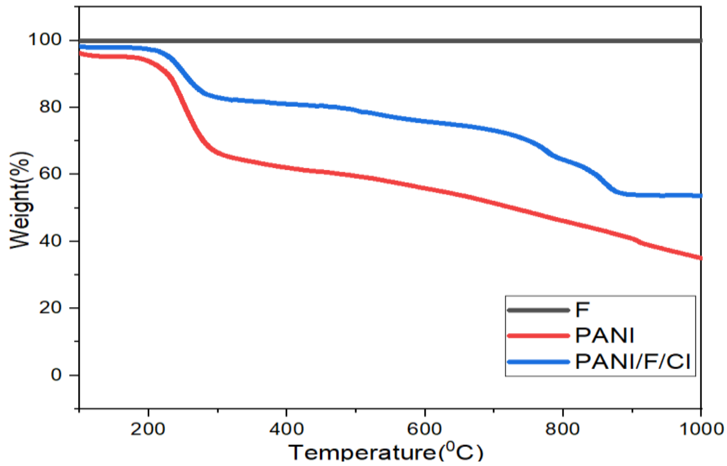

Figure 4. TGA thermograms of $Ni_{0.5}Zn_{0.5}Fe_2O_4$, PANI/F/CI composite and pure PANI

Morphology investigations

Figure 5 designates the morphology of the $Ni_{0.5}Zn_{0.5}Fe_2O_4$, CI, PANI and PANI/F/CI composite. The agglomerated spherical particles of NiZn ferrite and the spherical particles of carbonyl iron (Figure 5*a*, *b*) are observed with average diameters to be ranging between 27–63 nm and 0.2–2.4 μm, respectively. While a combination of rough surface sheets and short rods connected to each other of PANI is noticed (Figure 5*c*), distributed in the range between 60–220 nm. On the other hand, after coating with polyaniline, a continued overlayer of PANI is created on the CI and $Ni_{0.5}Zn_{0.5}Fe_2O_4$ nanoparticles' surface (Figure 5*d*).

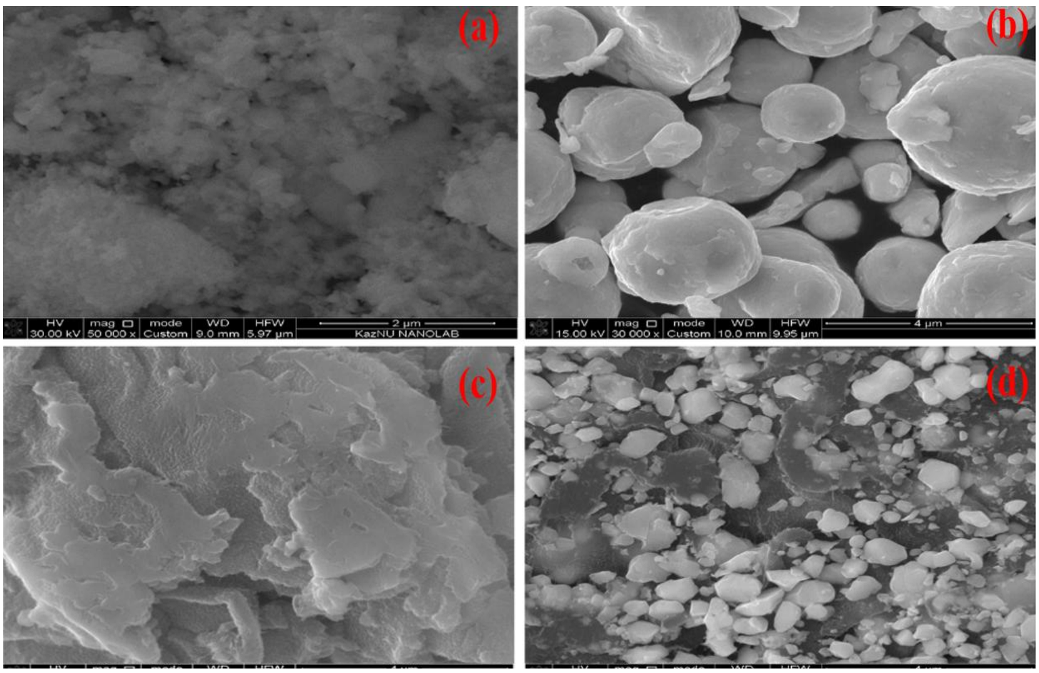

Figure 5. SEM images of (*a*) $Ni_{0.5}Zn_{0.5}Fe_2O_4$, (*b*) CI, (*c*) PANI and (*d*) PANI/F/CI composite

Energy-dispersive X-ray spectroscopy (EDX) analysis

Figure 6 and Table 1 present the energy-dispersive X-ray spectroscopy (EDX) analysis of $Ni_{0.5}Zn_{0.5}Fe_2O_4$, PANI and PANI/F/CI composite. The presence of C, O, Cl, S, Fe, Ni, Al, and Zn elements in the NiZn ferrite EDX spectrum is noticed. On the other hand, the presence of C, O, S and Cl elements in the PANI EDX spectrum is found. The presence of elemental Cl and S can be attributed to doping agents' hydrochloric acid and sodium dodecyl sulfate. Finally, the presence of C, O, Cl, S, Fe, Zn, Al, and Ni elements in the PANI/F/CI composite EDX spectrum is observed.

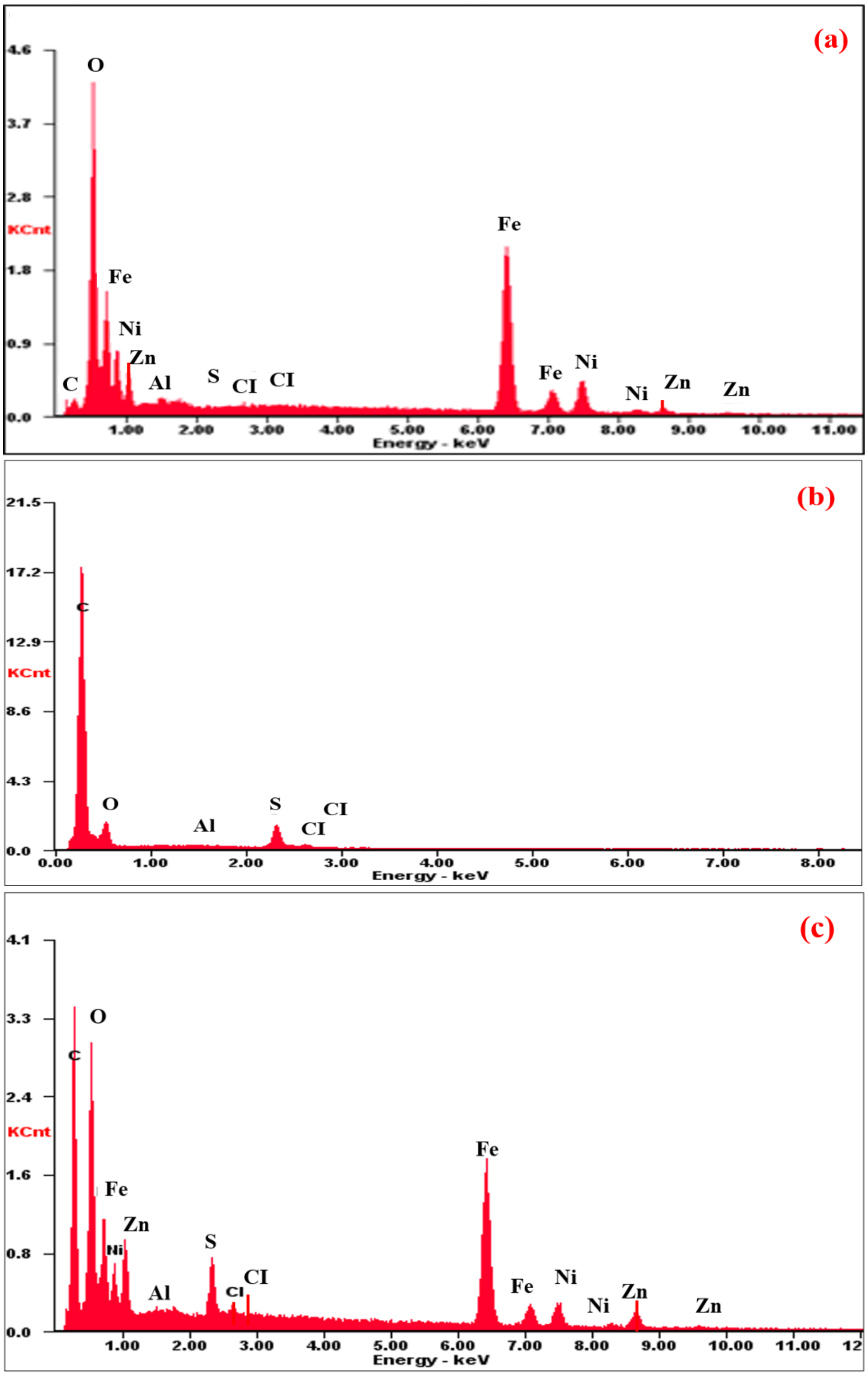

Figure 6. EDX of (*a*) $Ni_{0.5}Zn_{0.5}Fe_2O_4$, (*b*) PANI and (*c*) PANI/F/CI composite

Table 1

EDX element composition of $Ni_{0.5}Zn_{0.5}Fe_2O_4$, PANI and PANI/F/CI composite

Element	C	Cl	O	S	Al	Fe	Ni	Zn
Ferrite (wt %)	3.30	0.13	19.26	0.02	0.41	53.02	13.04	10.82
PANI (wt %)	84.52	0.45	11.81	3.17	0.05	0	0	0
PANI/F/CI (wt %)	51.72	0.51	19.23	2.02	0.08	17.15	5.32	3.97

MA and EMI shielding properties

MA and EMI shielding properties of the prepared samples are estimated with the free-space technique as illustrated in the following literature [27–31]. SE is calculated for the EMI shielding by applying the equation (1) [32]:

$$SE\left(dB\right) = SE_R + SE_A + SE_M = 10\log\frac{p_{in}}{p_T}, \tag{1}$$

where p_{in} and p_T — the incident power and transmitted power of the EM waves, respectively.

It is significant to note that the multiple reflection loss (SE_M) can be ignored if the absorption shielding (SE_A) of EMI shielding material is higher than 10 dB and equation (1) then can be rewritten as [32]:

$$SE\left(dB\right) = SE_R + SE_A = 10\ log\frac{p_{in}}{p_T}. \tag{2}$$

The shielding by reflection (SE_R) is calculated for the EMI shielding by applying the equation (3):

$$SE_R\left(dB\right) = -10\log\left(1-R\right) = -10\log\left(1-\frac{p_{ref}}{p_{in}}\right). \tag{3}$$

The shielding by absorption (SE_A) is calculated by equation (4) [33, 34]:

$$SE_A\left(dB\right) = -10\log\left(\frac{T}{1-R}\right) = -10\log\left(\frac{p_T}{p_{in}-p_{ref}}\right), \tag{4}$$

where p_{ref} — the reflected power of the EM waves.

On the other hand, *RL* is calculated for the MA by applying the equation (5) [33, 34]:

$$Rl\left(dB\right) = 10\log\frac{p_{in}}{p_{ref}}. \tag{5}$$

Influence of the incorporation of $Ni_{0.5}Zn_{0.5}Fe_2O_4$, CI and PANI on the RL and the SE

EMI shielding and MA properties of the $Ni_{0.5}Zn_{0.5}Fe_2O_4$, CI, PANI and PANI/F/CI composite are studied. The results of this investigation are exhibited in Figures 7, 8 and Table 2. Figures 7, 8 illustrate the changing of the RL and SE as a function of the EM wave frequency for $Ni_{0.5}Zn_{0.5}Fe_2O_4$, CI, PANI and PANI/F/CI composite. The absorption of samples with specified thickness at 3.2 mm is molded to measure RL and SE in the frequency band of 8.8–12.0 GHz. As illustrated in Figures 7, 8, a weak reflection loss and low shielding efficiency for the $Ni_{0.5}Zn_{0.5}Fe_2O_4$ and CI are noticed. On the other hand, for the pure PANI, the reflection loss is in the range between 6.6–8.5 dB and the shielding efficiency is in the range between 9.8–12.9 dB. Furthermore, when PANI is incorporated with ferrite which is mixed with carbonyl iron, the reflection loss increases to –25.8 dB at 11.3 GHz for PANI/F/CI composite and the shielding efficiency increases to 30.12 dB at 11.0 GHz. Table 2 shows the reasonable surface density (SD) of all the prepared absorbers. As a result, one can notice the impact of incorporating $Ni_{0.5}Zn_{0.5}Fe_2O_4$ and CI (magnetic loss materials) and PANI (dielectric loss material) on the EMI and MA properties of the prepared absorber. This incorporation leads to an effective and low thickness absorber with a wide BW_{-10dB} [35]. Figure 9 shows the SE_R and SE_A of the $Ni_{0.5}Zn_{0.5}Fe_2O_4$, CI, PANI and PANI/F/CI composite with a thickness of 3.2 mm at the frequency of 11.0 GHz.

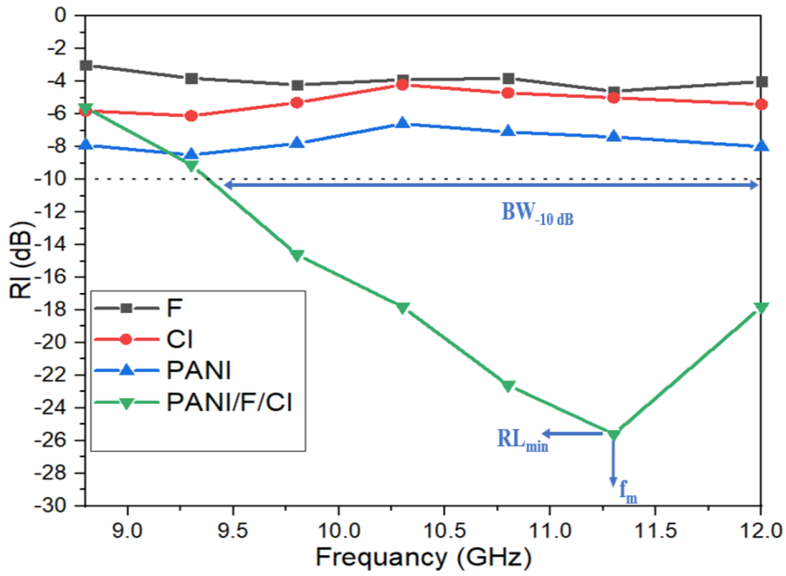

Figure 7. RL curves of $Ni_{0.5}Zn_{0.5}Fe_2O_4$, CI, PANI and PANI/F/CI composite at 3.2 mm thickness

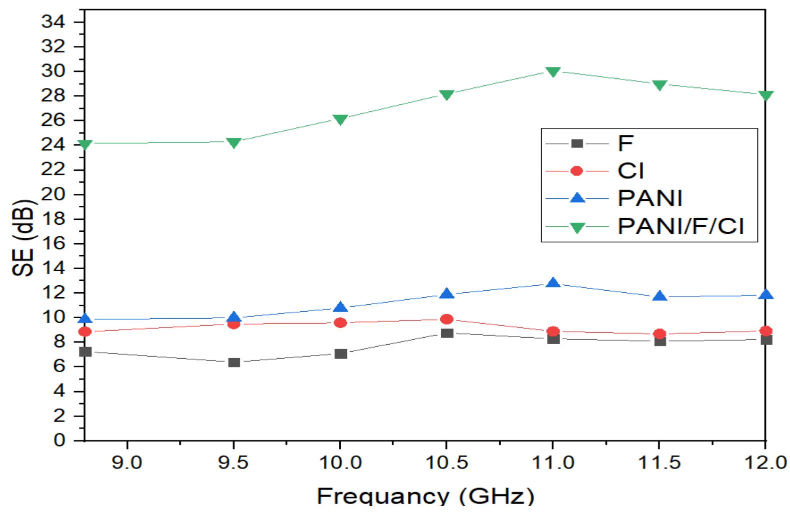

Figure 8. SE curves of $Ni_{0.5}Zn_{0.5}Fe_2O_4$, CI, PANI and PANI/F/CI composite at 3.2 mm thickness.

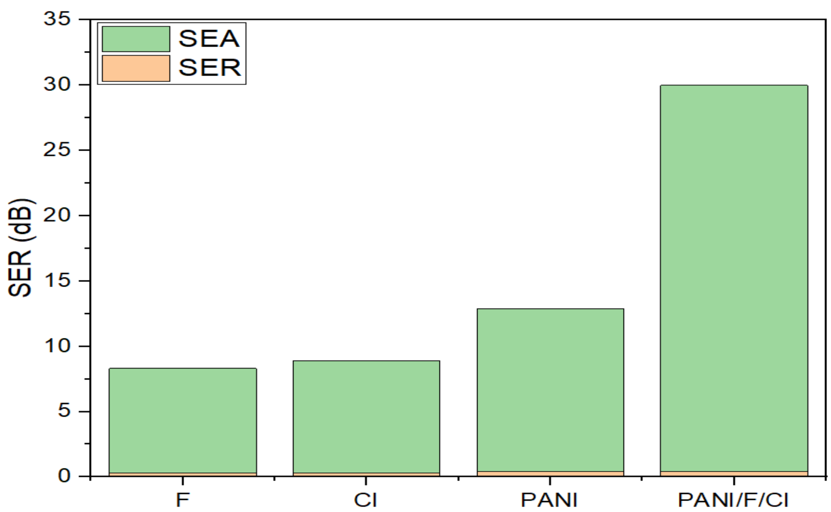

Figure 9. Bar plot for individual components of SE_R and SE_A of $Ni_{0.5}Zn_{0.5}Fe_2O_4$, CI, PANI and PANI/F/CI composite with a thickness of 3.2 mm at the frequency of 11.0 GHz

Table 2

MA behavior of $Ni_{0.5}Zn_{0.5}Fe_2O_4$, CI, PANI and PANI/F/CI composite at 3.2 mm thickness

Samples	RL_{min} (dB)	f_m (GHz)	$BW_{-10\ dB}$ (GHz)	SD (kg/m^2)
$Ni_{0.5}Zn_{0.5}Fe_2O_4$	–4.6	–	–	4.56
CI	–6.5	–	–	5.21
PANI	–8.5	–	–	2.25
PANI/F/CI	–25.7	11.3	2.6	3.31

Influence of the PANI/F/CI composite thickness and loading ratio on the RL

Figure 10 illustrates the RL of PANI/F/CI composite with various thicknesses (3.2, 3.4, 3.6 mm) at the various weight ratios of the absorber within a paraffin matrix (30, 35 % w/w). It can be seen that the RL attenuation peaks of samples moved to lower frequencies with increasing sample thickness. This phenomenon may be defined by the quarter-wavelength (λ/4) cancellation model, as shown in equation (6) [36–38]:

$$t_m = \frac{c}{4 f_m \sqrt{|\mu_r||\varepsilon_r|}}, \tag{6}$$

where $|\varepsilon_r|$ and $|\mu_r|$ are the modulus of the measured complex relative permittivity (ε_r) and permeability (μ_r) at matching frequency (f_m), respectively; c is the velocity of light.

It can be noticed from equation (6) that the f_m is inversely proportionate to the thickness of an absorber. On the other hand, one can notice the minimum reflection loss moves gradually to a lower frequency with the increase in weight ratios of the absorber within a paraffin matrix (Figure 10). Furthermore, Table 3 shows the PANI/F/CI composites have reasonable surface density, ranging from 3.31 to 3.40 kg/m^2, and wide bandwidth extending from 2.5 to 3.0 GHz. One can conclude that optimal absorption can be accomplished by modifying the absorber thickness and the loading ratio of the absorber within a paraffin matrix.

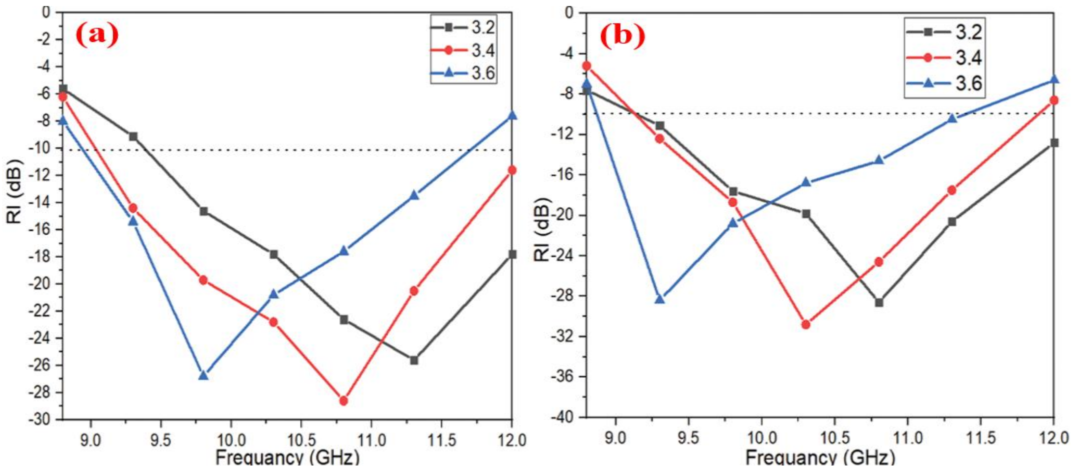

Figure 10. RL curves of PANI/F/CI composite with various thicknesses (3.2, 3.4, 3.6 mm) at the various weight ratios of the absorber within a paraffin matrix (*a*) 30 % and (*b*) 35 %

Table 3

MA behavior of PANI/F/CI composite at various thicknesses and various loading ratios within a paraffin matrix

Loading ratio %	t (mm)	RL_{min} (dB)	f_m (GHz)	BW_{-10dB} (GHz)	SD (kg/m^2)
30 %	3.2	–25.7	11.3	2.6	3.31
	3.4	–28.5	10.8	3.0	3.35
	3.6	–26.8	9.8	2.9	3.37
35 %	3.2	–28.6	10.8	2.5	3.33
	3.4	–30.8	10.3	2.8	3.38
	3.6	–28.4	9.3	2.6	3.40

To evaluate the beneficial impact of adding CI to the PANI/F on the microwave properties of the microwave absorber, Table 4 shows a comparison of MA properties of some lately reported PANI/NiZn ferrite absorbers with various loading ratios of the composites in the host matrix. Compared to PANI/NiZn ferrite absorbers reported by Ting et al. [3], Wang et al. and Wang et al. [7, 8], the current nanocomposite absorbers as-presented in this study display better MA in the frequency range of 8–12 GHz, lower loading ratio of the absorbers in the host matrix and relatively wider absorption bandwidth. However, the microwave absorber lately designed by Wang et al. [6] has comparable results with the current absorbers in terms of bandwidths and reflection losses, the lower loading ratios of the current absorbers are still an advantage. On the other hand, Didehban et al. designed absorbers with a low loading ratio similar to the ratio used in this study [5]. Although, the microwave properties of the current composites possess better reflection losses and larger bandwidths comparable with the result presented by Didehban et al. [5].

Table 4

Comparison of MA behavior of the current composites with similar absorbers in the literature

Specimen (relative weight ratio)/ host matrix	Loading percentage in the host matrix (%)	t (mm)	RL_{min} (dB)	f_m (GHz)	BW_{-10dB} (GHz)
PANI/F/CI/ Paraffin (current work)	30	3.4	–28.5	10.8	3.0
	35	3.4	–30.8	10.3	2.8
NiZn ferrite-PANI(50:50)/Epoxy [3]	67	2.00	–14	11.0	2.6
NiZn ferrite-PANI(35:65)/Epoxy [5]	20	2.00	–20	9.1	0.5
NiZn ferrite-PANI(1:3)/Paraffin [6]	75	3.50	–32	9.5	3.8
NiZn ferrite-PANI(2:1)/Paraffin [7]	70	2.00	–27.5	6.0	3.0
NiZn ferrite-PANI/Epoxy [8]	67	3.00	–17	11.1	2.8

These results prove that adding CI to the PANI/F has a beneficial role in enhancing the microwave properties of the absorber: It becomes lighter with wide bandwidth.

Conclusions

In the current research, we succeeded in the preparation of wideband and lightweight PANI/F/CI ferrite microwave absorbers with low loading ratios in paraffin wax 30–35 % w/w. The composites were structurally characterized using X-ray diffractometry, FTIR spectroscopy, UV-vis spectroscopy, and TGA. The morphology of the composites was investigated by scanning electron microscopy. The functional characterization was accomplished by measuring the EMI shielding and MA properties. The results show that by adequate control of the loading ratio and thickness of the absorber, one can tailor the design of a wideband and lightweight absorber based on PANI/F/CI in the frequency band of 8.8–12 GHz. Minimal reflection loss of –30.8 dB at the matching frequency of 10.3 GHz and the absorption bandwidth under –10 dB of 2.8 GHz for 3.4 mm thickness with a surface density of 3.38 kg/m^2 were noticed for the PANI/F/CI microwave absorber. The maximum shielding efficiency of 30.12 dB at 11.0 GHz for 3.2 mm thickness was observed for the PANI/F/CI microwave absorber.

References

1 Xie, X. B., Wang, B., Wang, Y., Ni, C., Sun, X., & Du, W. (2022). Spinel structured MFe_2O_4 (M = fe, co, ni, Mn, Zn) and their composites for microwave absorption: A Review. *Chemical Engineering Journal*, *428*, 131160. https://doi.org/10.1016/j.cej.2021.131160

2 Bera, P., Lakshmi, R. V., Prakash, B. H., Tiwari, K., Shukla, A., Kundu, A. K., Biswas, K., & Barshilia, H. C. (2020). Solution combustion synthesis, characterization, magnetic, and dielectric properties of $CoFe_2O_4$ and $Co_{0.5}M_{0.5}Fe_2O_4$ (M = Mn, Ni, and Zn). *Physical Chemistry Chemical Physics, 22*(35), 20087–20106. https://doi.org/10.1039/d0cp03161e

3 Ting, T. H., Yu, R. P., & Jau, Y. N. (2011). Synthesis and microwave absorption characteristics of polyaniline/NiZn ferrite composites in 2–40 GHz. *Materials Chemistry and Physics*, *126*(1-2), 364–368. https://doi.org/10.1016/j.matchemphys.2010.11.011

4 Houbi, A., Aldashevich, Z. A., Atassi, Y., Bagasharova Telmanovna, Z., Saule, M., & Kubanych, K. (2021). Microwave absorbing properties of ferrites and their composites: A Review. *Journal of Magnetism and Magnetic Materials*, *529*, 167839. https://doi.org/10.1016/j.jmmm.2021.167839

5 Didehban, K., Yarahmadi, E., Nouri-Ahangarani, F., Mirmohammadi, S. A., & Bahri-Laleh, N. (2015). Radar absorption properties of $Ni_{0.5}Zn_{0.5}Fe_2O_4$/pani/epoxy nanocomposites. *Journal of the Chinese Chemical Society, 62*(9), 826–831. https://doi.org/10.1002/jccs.201500136

6 Wang, M., Ji, G., Zhang, B., Tang, D., Yang, Y., & Du, Y. (2015). Controlled synthesis and microwave absorption properties of $Ni_{0.6}Zn_{0.4}Fe_2O_4$/Pani composite via an in-situ polymerization process. *Journal of Magnetism and Magnetic Materials, 377*, 52–58. https://doi.org/10.1016/j.jmmm.2014.10.066

7 Wang, C.-P., Li, C.-H., Bi, H., Li, J.-C., Zhang, H., Xie, A.-J., & Shen, Y.-H. (2014). Novel One-dimensional polyaniline/$Ni_{0.5}Zn_{0.5}Fe_2O_4$ hybrid nanostructure: Synthesis, magnetic, and electromagnetic wave absorption properties. *Journal of Nanoparticle Research*, *16*(3). https://doi.org/10.1007/s11051-014-2289-2

8 Wang, C., Shen, Y., Wang, X., Zhang, H., & Xie, A. (2013). Synthesis of novel Nizn-Ferrite/polyaniline nanocomposites and their microwave absorption properties. *Materials Science in Semiconductor Processing*, *16*(1), 77–82. https://doi.org/10.1016/j.mssp.2012.06.015

9 Ma, R.T., Zhao, H.T., & Zhang, G. (2010). Preparation, characterization and microwave absorption properties of polyaniline/$Co_{0.5}Zn_{0.5}Fe_2O_4$ nanocomposite. *Materials Research Bulletin*, *45*(9), 1064–1068. https://doi.org/10.1016/j.materresbull.2010.06.021

10 Chen, N., & Gu, M. (2012). Microstructure and microwave absorption properties of y-substituted Ni-Zn Ferrites. *Open Journal of Metal*, *02*(02), 37–41. https://doi.org/10.4236/ojmetal.2012.22006

11 Almessiere, M. A., Slimani, Y., Trukhanov, A. V., Demir Korkmaz, A., Guner, S., Akhtar, S., Shirsath, S. E., Baykal, A., & Ercan, I. (2020). Effect of ND-y co-substitution on structural, magnetic, optical and microwave properties of NICUZN nanospinel ferrites. *Journal of Materials Research and Technology*, *9*(5), 11278–11290. https://doi.org/10.1016/j.jmrt.2020.08.027

12 Almessiere, M.A., Slimani, Y., Güngüneş, H., Kostishyn, V.G., Trukhanov, S.V., Trukhanov, A.V., & Baykal, A. (2020). Impact of Eu^{3+} ion substitution on structural, magnetic and microwave traits of Ni–Cu–Zn spinel ferrites. *Ceramics International*, *46*(8), 11124–11131. https://doi.org/10.1016/j.ceramint.2020.01.132

13 He, J., Deng, L., Luo, H., He, L., Shan, D., Yan, S., & Huang, S. (2019). Electromagnetic matching and microwave absorption abilities of Ti_3SiC_2 encapsulated with $Ni_{0.5}Zn_{0.5}Fe_2O_4$ Shell. *Journal of Magnetism and Magnetic Materials*, *473*, 184–189. https://doi.org/10.1016/j.jmmm.2018.10.061

14 Niu, B., Zhang, F., Ping, H., Li, N., Zhou, J., Lei, L., Xie, J., Zhang, J., Wang, W., & Fu, Z. (2017). Sol-gel autocombustion synthesis of nanocrystalline high-entropy alloys. *Scientific Reports*, *7*(1). https://doi.org/10.1038/s41598-017-03644-6

15 El Nahrawy, A. M., Salah El-Deen, H., Soliman, A. A., & Mosa, W. M. M. (2018). Crystallographic and magnetic properties of Al^{3+}Co-doped $NiZnFe_2O_4$ nano-particles prepared by sol-gel process. *Egyptian Journal of Chemistry*. https://doi.org/10.21608/ejchem.2018.4504.1397

16 Bahri-Laleh, N., Didehban, K., Yarahmadi, E., Mirmohammadi, S. A., & Wang, G. (2017). Microwave absorption properties of polyaniline/carbonyl iron composites. *Silicon*, *10*(4), 1337–1343. https://doi.org/10.1007/s12633-017-9609-y

17 Ezzati, S. N., Rabbani, M., Leblanc, R. M., Asadi, E., Ezzati, S. M., Rahimi, R., & Azodi-Deilami, S. (2015). Conducting, magnetic polyaniline/$Ba_{0.25}Sr_{0.75}Fe_{11}(Ni_{0.5}Mn_{0.5})O_{19}$ nanocomposite: Fabrication, characterization and application. *Journal of Alloys and Compounds*, *646*, 1157–1164. https://doi.org/10.1016/j.jallcom.2015.05.146

18 Meng, X., Zhu, Y., Xu, S., & Liu, T. (2016). Facile synthesis of shell–core polyaniline/SRFE12O19 composites and magnetic properties. *RSC Advances*, *6*(6), 4946–4949. https://doi.org/10.1039/c5ra22200a

19 Ali, N. N., Atassi, Y., Salloum, A., Charba, A., Malki, A., & Jafarian, M. (2018). Comparative study of microwave absorption characteristics of (polyaniline/NiZn ferrite) nanocomposites with different ferrite percentages. *Materials Chemistry and Physics*, *211*, 79–87. https://doi.org/10.1016/j.matchemphys.2018.02.017

20 Prasanna, G. D., Jayanna, H. S., Lamani, A. R., & Dash, S. (2011). Polyaniline/$CoFe_2O_4$ nanocomposites: A novel synthesis, characterization and magnetic properties. *Synthetic Metals*, *161*(21-22), 2306–2311. https://doi.org/10.1016/j.synthmet.2011.08.039

21 Kondawar, S. B., & Nandapure, A. I. (2014). Magnetic and electrical properties of zinc-substituted nickel ferrite reinforced conducting polyaniline nanocomposites. *Journal of the Chinese Advanced Materials Society*, *2*(3), 186–198. https://doi.org/10.1080/22243682.2014.934919

22 Abdel Rahim, M. (2017). Carbon supported mono- and bi-metallic dispersed thin film catalysts for oxygen electro-reduction reaction in acid medium. International Journal of Electrochemical Science, 7890–7910. https://doi.org/10.20964/2017.08.23

23 Kim, S. Y., Kwon, S. H., Liu, Y. D., Lee, J.-S., You, C.-Y., & Choi, H. J. (2013). Core–shell-structured cross-linked poly(glycidyl methacrylate)-coated carbonyl iron microspheres and their magnetorheology. *Journal of Materials Science*, *49*(3), 1345–1352. https://doi.org/10.1007/s10853-013-7818-3

24 Gairola, S. P., Verma, V., Kumar, L., Dar, M. A., Annapoorni, S., & Kotnala, R. K. (2010). Enhanced microwave absorption properties in polyaniline and nano-ferrite composite in X-band. *Synthetic Metals*, *160*(21-22), 2315–2318. https://doi.org/10.1016/j.synthmet.2010.08.025

25 Li, G., Yan, S., Zhou, E., & Chen, Y. (2006). Preparation of magnetic and conductive NiZn ferrite-polyaniline nanocomposites with core-shell structure. *Colloids and Surfaces A: Physicochemical and Engineering Aspects*, *276*(1-3), 40–44. https://doi.org/10.1016/j.colsurfa.2005.10.010

26 Li, L., Jiang, J., & Xu, F. (2007). Synthesis and ferrimagnetic properties of novel SM-substituted LiNi Ferrite–polyaniline nanocomposite. *Materials Letters*, *61*(4-5), 1091–1096. https://doi.org/10.1016/j.matlet.2006.06.061

27 You, K. Y. (2017). Materials characterization using microwave waveguide system. *Microwave Systems and Applications*. https://doi.org/10.5772/66230

28 Skocik, P., & Neumann, P. (2015). Measurement of complex permittivity in Free Space. *Procedia Engineering*, *100*, 100–104. https://doi.org/10.1016/j.proeng.2015.01.347

29 Tamyis, N., Ramli, A., & Ghodgaonkar, D. K. (n.d.). Free space measurement of complex permittivity and complex permeability of magnetic materials using open circuit and short circuit method at microwave frequencies. *Student Conference on Research and Development*. https://doi.org/10.1109/scored.2002.1033141

30 Fwen, W., Ping, S., Abd Malek, M. F., & Hasss, N. (2012). Alternatives for PCB laminates: Dielectric Properties' measurements at microwave frequencies. *Dielectric Material*. https://doi.org/10.5772/50718

31 Gonçalves, F., Pinto, A., Mesquita, R., Silva, E., & Brancaccio, A. (2018). Free-space materials characterization by reflection and transmission measurements using frequency-by-frequency and multi-frequency algorithms. *Electronics*, *7*(10), 260. https://doi.org/10.3390/electronics7100260

32 Verma, P., Bansala, T., Chauhan, S. S., Kumar, D., Deveci, S., & Kumar, S. (2021). Electromagnetic interference shielding performance of carbon nanostructure reinforced, 3D printed polymer composites. *Journal of Materials Science*, *56*(20), 11769–11788. https://doi.org/10.1007/s10853-021-05985-0

33 Bayat, M., Yang, H., Ko, F. K., Michelson, D., & Mei, A. (2014). Electromagnetic interference shielding effectiveness of hybrid multifunctional Fe_3O_4/carbon nanofiber composite. *Polymer*, *55*(3), 936–943. https://doi.org/10.1016/j.polymer.2013.12.042

34 Hong, Y. K., Lee, C. Y., Jeong, C. K., Lee, D. E., Kim, K., & Joo, J. (2003). Method and apparatus to measure electromagnetic interference shielding efficiency and its shielding characteristics in broadband frequency ranges. *Review of Scientific Instruments*, *74*(2), 1098–1102. https://doi.org/10.1063/1.1532540

35 Ali, N. N., Atassi, Y., Salloum, A., Malki, A., Jafarian, M., & Almarjeh, R. K. (2019). Lightweight broadband microwave absorbers of core–shell (polypyrrole/nizn ferrite) nanocomposites in the X-band: Insights on Interfacial Polarization. *Journal of Materials Science: Materials in Electronics*, *30*(7), 6876–6887. https://doi.org/10.1007/s10854-019-01002-y

36 Wang, S., Jiao, Q., Shi, Q., Zhu, H., Feng, T., Lu, Q., Feng, C., Li, H., Shi, D., & Zhao, Y. (2020). Synthesis of porous nitrogen-doped graphene decorated by γ-FE2O3 nanorings for enhancing microwave absorbing performance. *Ceramics International*, *46*(1), 1002–1010. https://doi.org/10.1016/j.ceramint.2019.09.064

37 Shu, R., Zhang, J., Guo, C., Wu, Y., Wan, Z., Shi, J., Liu, Y., & Zheng, M. (2020). Facile synthesis of nitrogen-doped reduced graphene oxide/nickel-zinc ferrite composites as high-performance microwave absorbers in the X-band. *Chemical Engineering Journal*, *384*, 123266. https://doi.org/10.1016/j.cej.2019.123266

38 Jaiswal, R., Agarwal, K., Kumar, R., Kumar, R., Mukhopadhyay, K., & Prasad, N. E. (2020). EMI and microwave absorbing efficiency of polyaniline-functionalized reduced graphene oxide/γ-Fe_2O_3/epoxy nanocomposite. *Soft Matter*, *16*(28), 6643–6653. https://doi.org/10.1039/d0sm00266f

А. Хуби, А.А. Жарменов, И. Атасси, Ж.Т. Бағашарова, С. Мырзалиева, Б.А. Кәрібаев

Парафинді балауыз матрицасында полианилинмен қапталған $Ni_{0.5}Zn_{0.5}Fe_2O_4$/CI композитінің синтезі және микротолқынды сіңіру қасиеттері

Полианилин/$Ni_{0.5}Zn_{0.5}Fe_2O_4$/карбонил темірінің үштік композиттері (PANI/F/CI) екі кезең арқылы дайындалды: алдымен, $Ni_{0.5}Zn_{0.5}Fe_2O_4$ золь-гель әдісімен; содан соң PANI/F/CI композиттері $Ni_{0.5}Zn_{0.5}Fe_2O_4$ және CI болған кезде PANI-ның in-situ полимерлеу әдісі қолданылған. Үлгілерді сипаттау үшін рентгендік дифрактометрия (XRD — X-ray diffractometry), Фурье түрлендіру инфрақызыл спектроскопиясы (FTIR — Fourier transform infrared), ультракүлгін-көрінетін спектроскопиясы және термогравиметриялық талдау (TGA — Thermogravimetric analysis) пайдаланылды. Ұнтақтардың морфологиясы сканерлеуші электронды микроскоппен (SEM — Scanning electron microscope) зерттелген. Электромагниттік кедергілерді (EMI — electromagnetic interference) қорғау және микротолқынды жұту (MA — microwave absorption) қасиеттері 8,8–12 ГГц жиілік диапазонында өлшенді. Нәтижелер микротолқынды сіңіру қасиеттері абсорбердің қалыңдығына және парафиндік матрицадағы абсорбердің жүктеме қатынасына байланысты екенін көрсетті. Қалыңдығы 3,4 мм, бетінің тығыздығы 3,38 кг/м^2 болатын PANI/F/CI композиттік үлгісі үшін 10,3 ГГц сәйкес жиілікте (f_m) ең аз кері жоғалуы –30,8 дБ және жұту жолағы үшін 2,8 ГГц кезінде –10 дБ-ден (BW_{-10dB}) төмен болатыны анықталды. 3,2 мм қалыңдықтағы PANI/F/CI композиттік үлгісі үшін 11,0 ГГц жиілікте 30,12 дБ максималды экрандау тиімділігі байқалды.

Кілт сөздер: полианилин, карбонилді темір, композиттер, шағылысу жоғалуы, абсорбциялық жолақ ені.

А. Хуби, А.А. Жарменов, И. Атасси, Ж.Т. Багашарова, С. Мырзалиева, Б.А. Карибаев

Синтез и микроволновые поглощающие свойства композита $Ni_{0.5}Zn_{0.5}Fe_2O_4$/CI, покрытого полианилином в парафиновой матрице

Тройные композиты полианилин/$Ni_{0.5}Zn_{0.5}Fe_2O_4$/карбонильное железо (PANI/F/CI) получены двумя стадиями: сначала методом золь–гель был получен $Ni_{0,5}Zn_{0,5}Fe_2O_4$, после этого был получен композит PANI/F/CI с использованием технологии полимеризации PANI в присутствии $Ni_{0.5}Zn_{0.5}Fe_2O_4$ и CI. Для характеристики образцов использовались рентгеновская дифрактометрия (XRD), инфракрасная спектроскопия с преобразованием Фурье (FTIR), спектроскопия в ультрафиолетовом и видимом (UV-vis) спектрах и термогравиметрический анализ (TGA). Морфологии порошков были исследованы с помощью сканирующего электронного микроскопа (СЭМ). Свойства экранирования электромагнитных помех и поглощения микроволн измерялись в полосе частот 8,8–12 ГГц для исследования микроволновых характеристик. Результаты относятся к тем свойствам поглощения микроволн, которые связаны с толщиной поглотителя и коэффициентом загрузки поглотителя в парафиновой матрице. Для композитного образца PANI/F/CI были определены, что на частоте согласования 10,3 ГГц (f_m) минимальные потери на отражение составляют –30,8 дБ и полоса поглощения ниже –10 дБ (BW_{-10dB}) на частоте 2,8 ГГц для толщины 3,4 мм с поверхностной плотностью 3,38 кг/м^2. Для образца композита PANI/F/CI с толщиной 3,2 мм наблюдалась максимальная эффективность экранирования 30,12 дБ на частоте 11,0 ГГц.

Ключевые слова: полианилин, карбонильное железо, композиты, потери на отражение, ширина полосы поглощения.

Information about authors*

Houbi, Anas (*corresponding author*) — 3rd year PhD student, Department of Chemical Technology of Inorganic Substances, Al-Farabi Kazakh National University, Al-Farabi street, 71, 050040, Almaty, Kazakhstan; e-mail: anashoubi@gmail.com; https://orcid.org/0000-0001-9282-774X

Zharmenov, Abdurassul Aldashevich — General Director of the RSE “National Center on Complex Processing of Mineral Raw Materials of the Republic of Kazakhstan”, Dr. Sci. (Eng.), Prof., academician of the NAS of RK, State Premium Double Laureate, Jandossov street, 67, 050036, Almaty, Kazakhstan; e-mail: nc@cmrp.kz; https://orcid.org/ 0000-0001-5651-5343

Atassi, Yomen — Professor of Chemistry of Materials, Director of Materials Science Laboratory, Higher Institute for Applied Science and Technology (HIAST), Barzeh street, Damascus, Syria; e-mail: yomen.atassi@gmail.com; https://orcid.org/ 0000-0002-1338-4993

Bagasharova, Zhenisgul Telmanovna — Candidate of Technical Sciences, RSE “National center for complex processing of mineral raw materials of the Republic of Kazakhstan”, Senior Lecturer at Al-Farabi Kazakh National University, Al-Farabi street, 71, 050040, Almaty, Kazakhstan; e-mail: zh.t_bagasharova@mail.ru; https://orcid.org/0000-0001-8996-8656

Mirzalieva, Saule — Doctor of Chemical Sciences, Professor, Head of Department for Training of Scientific Personnel National Center for Complex Processing of Mineral Raw Materials of the Republic of Kazakhstan, Professor at Al-Farabi Kazakh National University, Al-Farabi street, 71, 050040, Almaty, Kazakhstan; e-mail: saulekerchaiz@mail.ru; https://orcid.org/0000-0003-2997-0716

Karibayev, Beibit Abdirbekovich — Acting Assistant Professor of Physics and Technology, Al-Farabi Kazakh National University, Al-Farabi street, 71, 050040, Almaty, Kazakhstan; e-mail: beibitkaribaev7@gmail.com; https://orcid.org/0000-0003-1057-0296

*The author’s name is presented in the order: *Last Name, First and Middle Names*